

## Electron Spin Resonance of Proton-Irradiated Graphite

Kyu Won Lee and Cheol Eui Lee\*

*Department of Physics and Institute for Nano Science, Korea University, Seoul 136-713, Korea*  
(Received 31 May 2005; revised manuscript received 13 June 2006; published 28 September 2006)

In the case of colossal magnetoresistance in the perovskite manganites, “double exchange” mediated by the itinerant spins is believed to play a key role in the ferromagnetism. In contrast, the conventional “Heisenberg” interaction, i.e., direct (unmediated) interaction between the localized spins produced by the proton irradiation, is identified as the origin of proton irradiation-induced ferromagnetism in graphite.

DOI: [10.1103/PhysRevLett.97.137206](https://doi.org/10.1103/PhysRevLett.97.137206)

PACS numbers: 75.50.Dd, 76.30.Lh, 76.30.Pk, 78.70.-g

This work was stimulated by the recent reports of ferromagnetism induced by proton irradiation in highly oriented pyrolytic graphite (HOPG) [1–4]. The proton irradiation studies in HOPG reveal that ferromagnetism in carbon-based materials, with a Curie temperature well above the room temperature, is closely related to the hydrogens adsorbed, opening a possibility for the micro-patterned ferromagnets of light elements. Helium-ion irradiation produced a very weak magnetic signal contrasting with the case of proton irradiation, indicating a decisive role of hydrogen [4], which was supported by some theoretical works [5,6]. In particular, hydrogenated graphite was theoretically predicted to display spontaneous magnetization arising from different numbers of mono- and double-hydrogenated carbon atoms [5]. Hydrogen adsorption on the irradiation-induced carbon vacancy was theoretically predicted to give rise to a magnetic moment double that of the naked vacancy [6]. Ferromagnetism was also observed in other forms of carbon-based materials, such as amorphous carbon and C60 polymers [7–9]. In a hydrogen-free carbon nanofoam with hyperbolically curved graphitic sheets, ferromagneticlike behaviors were observed [10], which indicates that different forms of carbon-based materials other than HOPG may have different origins of the ferromagnetism [10–12].

While it is evident that hydrogen plays a decisive role in the ferromagnetism in graphite, details of the magnetic ordering remain unclear. The magnetic resonance method is very useful for studying the microscopic details of the magnetic ordering, for which the electron spin resonance (ESR) measurements were carried out in this work. In fact, ESR in graphite has long been studied [13–17]. While the ESR line shape in graphite is of a Dysonian form originating from the conduction carriers [18], a strong scattering between the electrons and the holes is expected to give a single resonance line. The ESR intensity of the conduction electrons, which is proportional to the Pauli paramagnetic susceptibility, was observed to increase with temperature and was well described by the charge-carrier concentration calculated from the semimetallic band structure of graphite [13,19]. The large  $g$ -value anisotropy

observed, whose explanation has been attempted in view of the spin-orbit coupling, remains unexplained until now [13,16,17,20,21]. Small doping with ionized impurities [13,15] and neutron irradiation [14] gave no additional ESR signals other than the Dysonian line intrinsic to the pristine graphite, only giving rise to a reduction in the  $g$ -value anisotropy. Because the doping or the neutron irradiation produce the charge carriers causing a change in the Fermi level, the degeneracy in the energy bands at the zone edge was considered to be related to the large anisotropy of the  $g$  value [13–15]. While some ESR works for the carbon-based materials suggested an exchange interaction between the conduction electrons and the localized spins originating from the impurities or from irradiation, giving a modification in the ESR line shape [22–24], the ESR line of a neutron-irradiated graphite single crystal showed the characteristic Dysonian shape as mentioned above [14].

The HOPG (ZYA grade, with a content of magnetic metallic impurities below 1 ppm) samples of dimensions  $2.5 \times 2.5 \times 0.4 \text{ mm}^3$ , purchased from the Structure Probe, Inc., were irradiated with a 2.25-MeV proton beam of a spot radius 0.5 cm to a dose of  $1.875 \times 10^{17} \text{ ions/cm}^2$  at room temperature. The magnetization was measured employing a superconducting quantum interference device (SQUID) magnetometer (Quantum Design MPMS series). A JEOL JES-FA200 spectrometer was used for the ESR experiment at 9 GHz. Before the irradiation, only the  $G$  (graphitic) band was observed in the Raman spectrum at room temperature, whereas after the irradiation, the  $D$  (disorder) band appeared in addition to the  $G$  band, with an areal fraction  $D/G \sim 1/5$ .

Figure 1(a) shows the magnetization measured at 5 K with the magnetic field perpendicular to the  $c$  axis before and after the irradiation. The irradiation-induced magnetization, obtained by subtracting the magnetization of the raw sample from that of the irradiated sample, shows a paramagnetic behavior, being linear to the applied field without saturation up to 1 T. Figure 1(b) shows the magnetization measured at 5 K with the magnetic field parallel to the hexagonal  $c$  axis before and after the irradiation. The

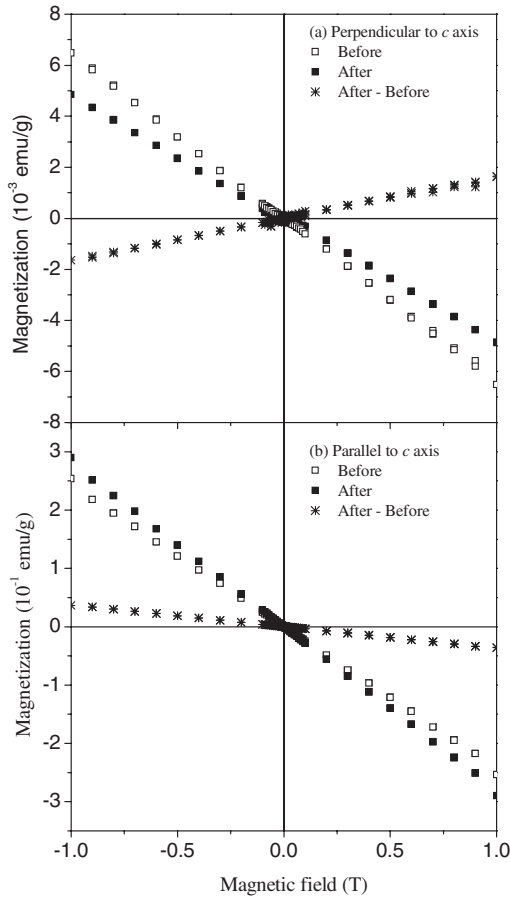


FIG. 1. The magnetization measured at 5 K (a) with the magnetic field perpendicular to the  $c$  axis and (b) with the magnetic field parallel to the  $c$  axis. \* represents the residual magnetization obtained by subtracting the magnetization of the raw sample from that of the irradiated sample.

diamagnetism observed with the magnetic field parallel to the  $c$  axis is due to a Landau diamagnetism, for which the charge carriers move in quantized orbits. The additional diamagnetic contribution would thus indicate an increase in the carrier concentration.

Figure 2 shows the ESR spectra before and after the irradiation, measured at 300 K with the magnetic field rotated from the  $ab$  plane to the  $c$  axis. Before the irradiation [Fig. 2(a)], the ESR line shape is a Dysonian form indicating a conducting behavior of the HOPG, with a large  $g$ -value anisotropy. The  $g$  value of the HOPG shows the same angular dependence as previously reported [13]:  $g = g_{\text{per}} + A \cos^2 \theta$ , where  $g_{\text{per}} \sim 2.002$ ,  $A \sim 0.047$ , and  $\theta$  correspond to the  $g$  value perpendicular to the  $c$  axis, the  $g$ -value anisotropy, and the angle between the magnetic field and the  $c$  axis, respectively.

Figure 3 shows the temperature evolution of the ESR spectra measured with the magnetic field perpendicular to the  $c$  axis. Before the irradiation, Fig. 3(a), the ESR intensity increased with increasing temperature as was reported in previous works [13,14,16,17]. In contrast, the

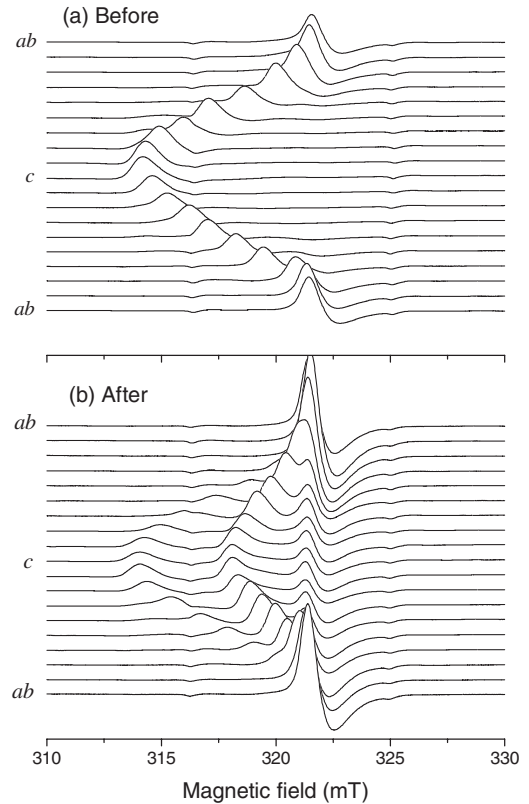


FIG. 2. ESR spectra (a) before and (b) after the irradiation, measured at 300 K with the magnetic field rotated from the  $ab$  plane to the  $c$  axis. The ESR peaks were labeled  $D1$ ,  $D2$ , and  $L1$ , in the direction of increasing resonance field.

ESR intensity after the irradiation, shown in Fig. 3(b), decreased with increasing temperature below 270 K.

The ESR signal observed in the irradiated sample arises from the localized paramagnetic moments as well as the conduction electrons, which are well separated in the ESR spectra measured with the magnetic field parallel to the  $c$  axis [Fig. 2(b)]. While various forms of hydrogen-adsorbed defects were suggested as origins of the localized magnetic moment [6], no hyperfine structure was apparent in our ESR spectra, which can be taken as a negative evidence for the hydrogen-adsorbed defects as an origin of the magnetic moment.

The ESR spectra measured with the magnetic field parallel to the  $c$  axis show a fairly complicated form as shown in Fig. 2(b) and 4, composed of at least three distinct peaks. In the direction of increasing resonance field, the peaks were labeled  $D1$ ,  $D2$ , and  $L1$  (shown in Fig. 4), of which  $D1$  and  $D2$  are Dysonian-like and  $L1$  is Lorentzian-like. The Dysonian line shapes of  $D1$  and  $D2$  indicate that they arise from the conduction electrons, whereas the Lorentzian line  $L1$  is attributed to the localized magnetic moments. As shown in Figs. 2(b) and 4, the resonance field of  $L1$  is independent of temperature as well as the angle between the magnetic field and the  $c$  axis. The intensity of

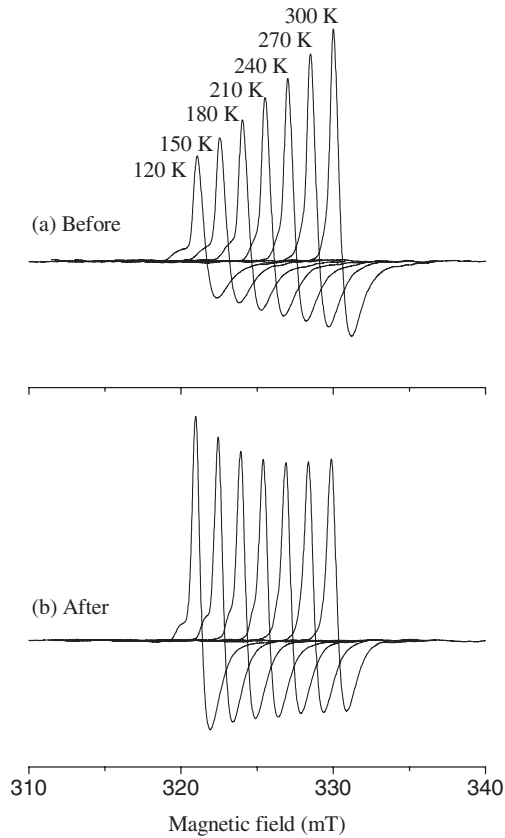


FIG. 3. Temperature evolution of the ESR spectra (a) before and (b) after the irradiation, measured with the magnetic field perpendicular to the  $c$  axis. The resonance field exhibited virtually no temperature dependence, the spectra being displaced equidistantly for a clear display.

$L1$  decreasing with increasing temperature also suggests that  $L1$  arises from the isolated paramagnetic moments.

The Dysonian line  $D1$  showed the same temperature and angle dependence as those of the ESR spectrum measured before the irradiation, which indicates that the line corresponds to the carriers arising from the semimetallic band structure of the pristine graphite. As the penetration depth of the 2.25-MeV proton is  $\sim 50 \mu\text{m}$  [1] while our sample thickness is  $\sim 400 \mu\text{m}$ ,  $D1$  can be ascribed to the graphite region unaffected by the irradiated protons. While thin enough samples of HOPG may be used in order to probe fully irradiated samples to remove the  $D1$  line and to prove that our  $D2$  line is the one due to irradiation, they would suffer from warping and roughening, all of which can give rise to unwanted magnetic moments. Nonetheless, as we peeled off the unirradiated side of the irradiated HOPG, the  $D1$  line intensity was observed to decrease. A simple comparison of the ESR spectra before and after the irradiation (Fig. 2) is enough to show that the  $D1$  line belongs to the unirradiated HOPG and the other lines belong to the irradiated HOPG.

The Dysonian line  $D2$  showed an angle dependence similar to that of  $D1$ , with the  $g$ -value anisotropy reduced

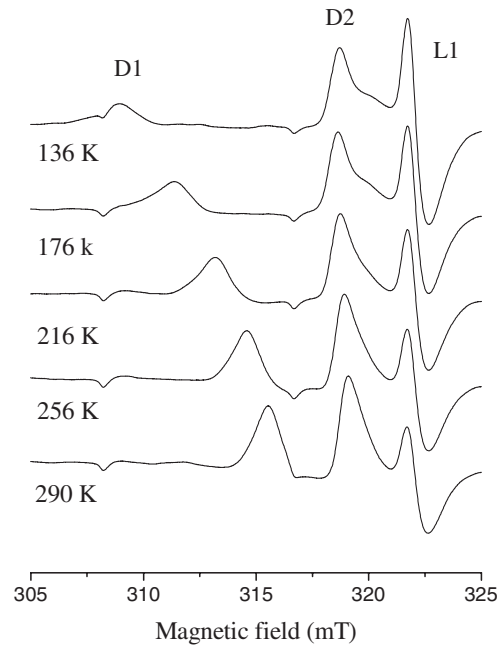


FIG. 4. Temperature evolution of the ESR spectra after the irradiation, measured with the magnetic field parallel to the  $c$  axis. The small dips in the spectra are the Mn marker signals.

by a half. The ESR intensity and the resonance field of  $D2$  were nearly independent of temperature, indicating that the line can be attributed to the carriers arising from the metal-like band structure. The reduction in the  $g$ -value anisotropy was also observed in doped graphite with ionized impurities [13,15]. Neutron irradiation in graphite was also reported to produce additional mobile holes, decreasing the ESR  $g$ -value anisotropy [14]. Thus,  $D2$  may unambiguously be ascribed to the carriers in the proton-irradiated graphite.

In the McClure-Yafet's early theory [20], the  $g$ -value anisotropy becomes zero for two-dimensional graphite, owing to complete compensation of electron and hole contributions. Later, this conclusion was corrected by taking into account the contribution of the spin-orbit splitting of the Landau levels [16,21]. In a recent work, the  $g$ -value shift  $\Delta g = g - 2$  was given by  $\Delta g = -\Lambda\chi(T, H)/[\mu_B^2 N_{\text{eff}}(T, H)]$  [17].  $\Lambda$ ,  $\mu_B^2$ ,  $N_{\text{eff}}(T, H)$ , and  $\chi(T, H) = M(T, H)/H$  are the spin-orbit parameter, the Bohr magneton, effective electron density, and the electron orbital susceptibility, respectively. The large reduction in the  $g$ -value anisotropy after the irradiation with preserving the large susceptibility anisotropy indicates an increase in the effective carrier density.

It has been reported that a large number of localized spin centers and a small number of conduction carriers were produced by irradiation in the polycrystalline graphite and carbon nanotubes, where the two kinds of the spin centers were coupled by a strong exchange interaction giving a single Lorentzian-like ESR line [23,25,26]. This is con-

trasting to the single Dysonian line in a neutron-irradiated single crystal [14], and also to the two separate lines,  $D2$  and  $L1$ , in the proton-irradiated HOPG in this work. Because the edge state of a small-size graphite and the curvature of a graphitic sheet may induce magnetic moments [10,12], the irradiation effect in those forms of carbon-based materials may be different from that in a single crystal. A recent ESR study of hydrogen adsorption effects reported a reduced paramagnetic defect signal in the single-wall nanotubes and an enhanced Dysonian line in the multiwall carbon nanotubes [27]. In our proton-irradiated HOPG, the well-separated  $D2$  and  $L1$  lines with completely distinct temperature and angle dependencies would indicate that there is no exchange interaction between the carrier spins and the localized spins, so that the magnetic long range order would have to arise exclusively from the direct interaction between the localized spins, without a vital mediating role of the itinerant spins, which is believed to be the case in the colossal magnetoresistance in the perovskite manganites [28,29].

In summary, a systematic work employing magnetic and electron spin resonance measurements has been carried out in order to elucidate the origin of the ferromagnetism in proton-irradiated graphite. In addition to a Dysonian line with a reduced  $g$ -value anisotropy, attributed to a modification in the Fermi level for the carriers, a Lorentzian-like line without a  $g$ -value anisotropy, attributed to the irradiation-induced defects, was observed in the proton-irradiated graphite. The apparent absence of a hyperfine structure in our ESR spectra may be a negative evidence for the hydrogen-adsorbed defect as an origin of the magnetic moment. Our results indicate that direct interaction between the localized spins produced by the proton irradiation is the origin of the proton-irradiated ferromagnetism in graphite.

This research work was supported by the User Program of PEFP (Proton Engineering Frontier Project), as a part of the 21C Frontier R&D Program supported by the MOST (Ministry of Science and Technology).

---

\*Corresponding author.

Electronic address: rscel@korea.ac.kr

- [1] P. Esquinazi, D. Spemann, R. Hohne, A. Setzer, K.-H. Han, and T. Butz, *Phys. Rev. Lett.* **91**, 227201 (2003).
- [2] P. Esquinazi, A. Setzer, R. Hohne, C. Semmelhack, Y. Kopelevich, D. Spemann, T. Butz, B. Kohlstrunk, and M. Losche, *Phys. Rev. B* **66**, 024429 (2002).
- [3] D. Spemann, P. Esquinazi, R. Hohne, A. Setzer, M. Diaconu, H. Schmidt, and T. Butz, *Nucl. Instrum. Methods Phys. Res., Sect. B* (to be published).
- [4] K.H. Han, D. Spemann, P. Esquinazi, R. Hohne, V. Riede, and T. Butz, *Adv. Mater.* **15**, 1719 (2003).
- [5] K. Kusakabe and M. Maruyama, *Phys. Rev. B* **67**, 092406 (2003).
- [6] P.O. Lehtinen, A.S. Foster, Y. Ma, A.V. Krasheninnikov, and R.M. Nieminen, *Phys. Rev. Lett.* **93**, 187202 (2004).
- [7] K. Murata, H. Ushijima, H. Ueda, and K. Kawaguchi, *J. Chem. Soc. Chem. Commun.* **18**, 1265 (1991).
- [8] K. Murata, H. Ushijima, H. Ueda, and K. Kawaguchi, *J. Chem. Soc. Chem. Commun.* **7**, 567 (1992).
- [9] T.L. Makarova, B. Sundqvist, R. Hohne, P. Esquinazi, Y. Kopelevich, P. Scharff, V.A. Davydov, L.S. Kashevarova, and A.V. Rakhmanina, *Nature (London)* **413**, 716 (2001).
- [10] A.V. Rode, E.G. Gamaly, A.G. Christy, J.G. FitzGerald, S.T. Hyde, R.G. Elliman, B. Luther-Davies, A.I. Veinger, J. Androulakis, and J. Giapintzakis, *Phys. Rev. B* **70**, 054407 (2004).
- [11] A.A. Ovchinnikov and V.N. Spector, *Synth. Met.* **27**, 615 (1988).
- [12] K. Wakabayashi, M. Fujita, H. Ajiki, and M. Sigrist, *Phys. Rev. B* **59**, 8271 (1999).
- [13] G. Wagoner, *Phys. Rev.* **118**, 647 (1960).
- [14] K. Muller, *Phys. Rev.* **123**, 1550 (1961).
- [15] L.S. Singer and G. Wagoner, *J. Chem. Phys.* **37**, 1812 (1962).
- [16] K. Matsubara, T. Tsuzuku, and K. Sugihara, *Phys. Rev. B* **44**, 11 845 (1991).
- [17] D.L. Huber, R.R. Urbano, M.S. Sercheli, and C. Rettori, *Phys. Rev. B* **70**, 125417 (2004).
- [18] G. Feher and A.K. Kip, *Phys. Rev.* **98**, 337 (1955).
- [19] J.W. McClure, *Phys. Rev.* **108**, 612 (1957).
- [20] J.W. McClure and Y. Yafet, in *Proceedings of the Fifth Conference on Carbon*, edited by S. Mrozowsky and P.L. Walker (Pergamon, New York, 1962), Vol. 1, p. 22.
- [21] A.S. Kotosonov, *Carbon* **26**, 735 (1988).
- [22] J.H. Pifer and R.T. Longo, *Phys. Rev. B* **4**, 3797 (1971).
- [23] F. Beuneu, C. IHuillier, J.-P. Salvétat, J.-M. Bonard, and L. Forro, *Phys. Rev. B* **59**, 5945 (1999).
- [24] C. Buschhaus and E. Dormann, *Phys. Rev. B* **66**, 195401 (2002).
- [25] S. Mrozowski, *Carbon* **3**, 305 (1965).
- [26] S. Mrozowski, *Carbon* **6**, 243 (1968).
- [27] K. Shen, D.L. Tierney, and T. Peitross, *Phys. Rev. B* **68**, 165418 (2003).
- [28] C. Zener, *Phys. Rev.* **81**, 440 (1951); P. de Gennes, *Phys. Rev.* **118**, 41 (1960).
- [29] S. Jin, T.H. Tiefel, M. McCormack, R.A. Fastnacht, R. Ramesh, and L.H. Chen, *Science* **264**, 413 (1994).